New Antiplasmodial Bromotyrosine Derivatives from *Suberea ianthelliformis* LENDENFELD, 1888

by **Luke Mani**[a][b], **Valerie Jullian**[a], **Beatrice Mourkazel**[a], **Alexis Valentin**[a], **Joëlle Dubois**[c], **Thierry Cresteil**[c], **Eric Folcher**[d], **John N. A. Hooper**[e], **Dirk Erpenbeck**[f], **William Aalbersberg**[b], and **Cécile Debitus***[g]

[a]) UMR 152, IRD, 118, route de Narbonne, FR-31062 Toulouse cedex 9
[b]) University of the South Pacific, Laucala Campus, Suva, Fiji
[c]) UPR2301, CNRS, Institut de Chimie des Substances Naturelles, avenue de la terrasse, FR-91198 Gif sur Yvette Cedex
[d]) Service d'Exécution des Opérations Hyperbares, IRD, BPA5, 98713 Nouméa cedex, New Caledonia
[e]) Queensland Museum, P.O. Box 3300, South Brisbane bc, Queensland 4101, Australia
[f]) Department of Earth and Environmental Sciences & GeoBio-Center LMU, Ludwig-Maximilians-University Munich, Richard Wagner Str. 10, DE-80333 Munich
[g]) UMR 7138, IRD, BP529, 98713 Papeete, French Polynesia
(phone: +689-47-42-03; cecile.debitus@ird.fr)

Four samples of *Suberea ianthelliformis* were investigated and furnished five new and 13 known brominated tyrosine-derived compounds. Two of the new compounds were identified as araplysillin N20-formamide and its *N*-oxide derivative. Three other new compounds, araplysillins IV, V, and VI, were isolated and identified as analogs of araplysillin II. Most of these compounds exhibit moderate inhibitory activities against chloroquine-resistant and -sensitive strains of *Plasmodium falciparum*, and were investigated for their PFTase inhibitory properties. The chemical content of the investigated sponges is correlated with their molecular phylogeny.

Introduction. – Porifera, especially demosponges which represent over 85% of this phylum, have been and are still widely studied for drug discovery since the 1960's [1]: they remain one of the best source of new structures and bioactive marine natural products. Their way of life, as sessile organisms feeding on filtering water, leads to a high level of adaptability for surviving competitor, predator, and parasite pressure, especially through the production of secondary metabolites [2][3]. Some species are regarded as widely distributed, but recent genetic investigations showed that endemism and cryptic speciation occurs more frequently than initially expected, *e.g.* [4], which may also lead to chemical diversity, and give a new look to chemotaxonomy [5]. They are furthermore associated with a wide array of microorganisms, which contribute to a high-tech secondary metabolites machinery for the production of highly diversified libraries of compounds of all natural products series: lipids, terpenoids, alkaloids, peptides, macrolides, *etc.* These molecules often display typical marine characters, such as halogenated substituents, and have been designed during the evolution to reach their targets in highly diluted conditions, and are such among the most bioactive natural products. Many chemical skeletons are only found in marine organisms, especially in sponges, *e.g.*, amino-imidazole alkaloids of the Agelasidae [6], bromotyrosine

derivatives of the Verongida [7], or polyketides and peptides of some lithistid sponges [8]. The specific diversity, combined with the biogeographic diversity, leads to a rich chemodiversity in each series of compounds. They lead to a wide range of biosynthetic pathways which can be used to develop some high-yield biomimetic syntheses [9].

As a part of our investigation of South Pacific sponges, we analyzed four samples of Verongida from the Solomon Islands, all identified as *Suberea ianthelliformis*, in order to search for new antimalarial agents, and secondly for their utility as chemotaxonomic markers. Sponges have been relatively poorly explored for antimalarial compounds, but some promising agents have been discovered such as manzamine, phloeodictyne, or endoperoxidic terpenoids [10]. They display a rich source of diversified bioactive compounds against malaria but also against other major tropical parasitic diseases [11]. Only few bromotyrosine derivatives are yet described as antiparasitic compounds from verongid sponges [12][13]. The *Suberea ianthelliformis* extracts studied in this work were selected from the high-throughput screening of our library of Solomon Islands marine sponge EtOH crude extracts, with the aim to select more specific antimalarial agents by inhibition of protein farnesyltransferase, correlated with a differential cytotoxicity against KB cancer cell-lines and *Plasmodium falciparum*. Protein farnesyltransferases (PFTase) are enzymes that transfer 15-carbon isoprenyl units to many proteins, among which are heterotrimeric G-proteins – a trigger to a cascade of events leading to cell differentiation. Initially investigated as a target for anticancer chemotherapy, evidence that some mammalian PFTase inhibitors selectively arrest *Plasmodium falciparum* differentiation focused attention on PFTase as an antiplasmodial target [14–18].

Five new compounds, araplysillin N20-formamide (**2**) and its *N*-oxide derivative (**3**), and araplysillins IV, V, and VI (**5**–**7**, resp.), were characterized in this work. They were isolated from a complex mixture of bromotyrosine analogs. The chemical composition of the investigated sponges is discussed in relation to the bioactivity and molecular phylogeny of these samples. The isolated compounds of sponges *I* and *II* are shown in *Fig. 1* and those from sponge *III* in *Fig. 2*. Sponge *IV* did not provide any relevant compound.

Results and Discussion. – 1. *Chemistry.* Investigation of *Suberea ianthelliformis* sponges led to the isolation and identification of a meroterpenoid, aureole [19], a steroid, aplysinasterol [20], and ten known and five new bromotyrosine compounds (see *Table 1*). Only the structure determination of the five new bromotyrosine-derived compounds, related to araplysillins I (**1**) and II (**4**) [21], is discussed here, as well as the content of the investigated sponges towards molecular systematics, and the bioactivity of the known and of the new purified compounds.

Compound **2** was obtained as an optically active solid ($[\alpha]_D^{25} = -72$, $c = 0.01$, MeOH). The HR-DCI-MS (CH_4; positive-ion mode) spectrum displayed a 1:3:5:3:1 cluster of signals centered at *m/z* 767.8177 ($\Delta + 0.7$ mmu; $[M+Na]^+$), consistent with a tetrabrominated compound, indicating a molecular formula of $C_{22}H_{23}Br_4N_3O_6$ and possessing eleven degrees of unsaturation. The UV spectrum (λ_{max} at 220 nm (ε, 41800) and 285 nm (ε, 10450)) indicated the presence of a heteroatom-substituted cyclohexadienyl moiety, while the IR spectrum exhibited bands at 3307, 1733, 1659, and

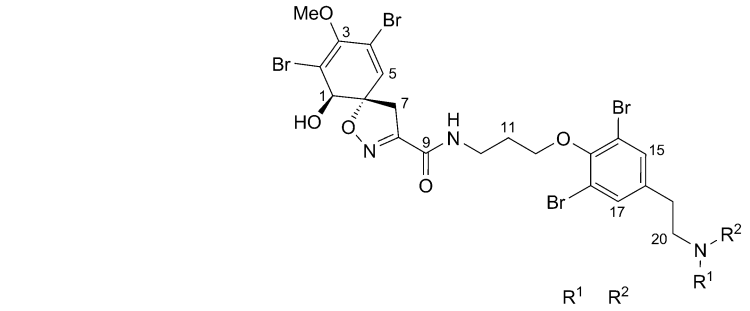

	R^1	R^2
Araplysillin I (**1**)	H	H
Araplysillin N20-formamide (**2**)	H	CHO
Araplysillin N20-hydroxyformamide (**3**)	OH	CHO
Araplysillin II (**4**)	H	$CO(CH_2)_{11}CHMe_2$
Araplysillin IV (**5**)	H	$CO(CH_2)_8CH(Me)(CH_2)_5Me$
Araplysillin V (**6**)	H	$CO(CH_2)_{10}CH(Me)(CH_2)_5Me$

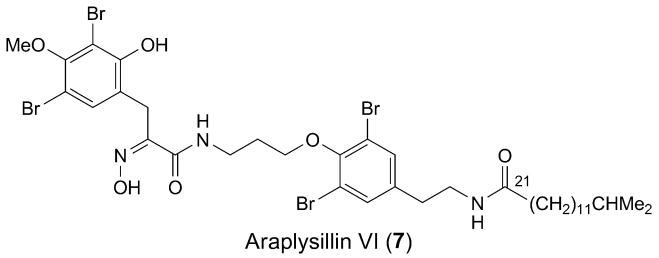

Araplysillin VI (**7**)

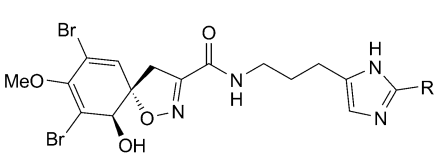

Aerophobin I (**8**) R = H
Aerophobin II (**9**) R = NH_2

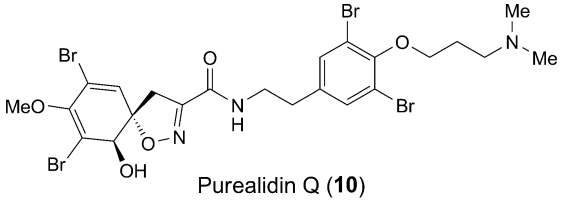

Purealidin Q (**10**)

Fig. 1. *Bromotyrosine-derived compounds identified from sponges* I *and* II

1534 cm^{-1} characteristic of alcohol, aldehyde, and α-iminoamide motifs, respectively [22].

Diagnostic signals in the ^{1}H-NMR spectrum (see *Table 2*) at δ(H) 6.35 (*s*), 4.41 (*s*), 3.74 (*s*), 3.05 (*d*, $J = 18.5$), and 3.94 (*d*, $J = 18.5$) suggested a MeO-substituted dibromo-spiro[cyclohexadien-isoxazole] moiety **A**, very common in verongid sponges [23–26]. The HMBCs of these H-atoms (*Fig. 3*, substructure **A**) confirmed the MeO-substituted dibromo-spiro[cyclohexadien-isoxazole] moiety.

The ^{1}H,^{1}H-COSY spectrum revealed an electron spin system δ(H) 4.10 (CH_2(12)), 2.13 (CH_2(11)), 3.70 (CH_2(10)), 7.16 (H–N–C(9)), consistent with an *O*-propylamine motif **B** (*Fig. 3*). The HMBC of δ(H) 3.70 to C(9) (δ(C) 159.0) suggested that the *O*-propylamine and isoxazole moieties were amide-linked. Such an amide link was

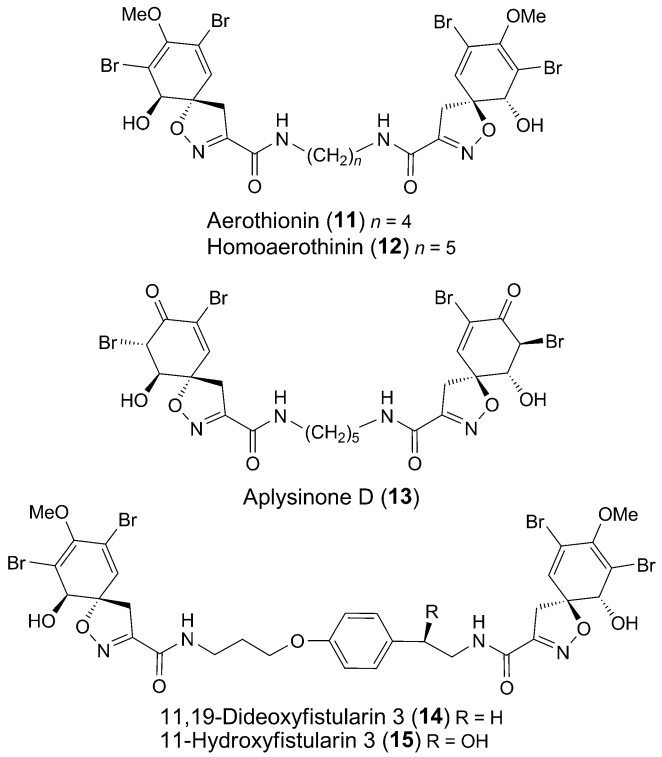

Fig. 2. *Bromotyrosine-derived compounds identified from sponge* III

Table 1. *Isolated Compounds* (mass, yield) *from* Suberea ianthelliformis *Sponges*

Source sponge	Known compounds	New compounds
I	Aureole (42 mg, 0.02%)	Araplysillin N20-formamide (**2**; 3.1 mg, 1.5 ppm)
	Aplysterol (67 mg, 0.032%)	Araplysillin IV (**5**; 3 mg, 1.4 ppm)
	Araplysillin I (**1**; 47 mg, 0.023%)	Araplysillin V (**6**; 2.3 mg, 1.1 ppm)
	Araplysillin II (**4**; 55 mg, 0.027%)	Araplysillin VI (**7**; 2.2 mg, 1 ppm)
II	Aerophobin I (**8**; 2 mg, 3.4 ppm)	Araplysillin N20-hydroxyformamide
	Aerophobin II (**9**; 23 mg, 0.039%)	(**3**; 3.1 mg, 5.2 ppm)
	Purealidin Q (**10**; 34 mg, 0.058%)	
III	Aerothionin (**11**; 72 mg, 0.035%)	
	Homoaerothionin (**12**; 102 mg, 0.049%)	
	11,19-Dideoxyfistularin 3 (**13**; 10 mg, 4.8 ppm)	
	11-Hydroxyfistularin (**14**; 14 mg, 6.7 ppm)	
	Aplysinone D (**15**; 9 mg, 4.3 ppm)	

supported by an IR absorbance band at 1659 cm^{-1}. The two-H-atom *singlet* at δ(H) 7.37 was in accordance with a symmetrically dibrominated aryl moiety. Additional, an ethylamide moiety, *i.e.*, R–CH_2CH_2NHCHO, was revealed by the spin system δ(H)

Table 2. *NMR Spectroscopic Data for Araplysillin N20-Formamide* (**2**; in $CDCl_3$) *and Araplysillin N20-Hydroxyformamide* (**3**; in CD_3OD). ^{1}H-NMR Spectra were measured at 125 MHz, and ^{13}C-NMR spectra at 500 MHz, resp.

	2			**3**	
	δ(H)	δ(C)	HMBC	δ(H)	δ(C)
H–C(1)	4.41 (*s*)	74.0 (*d*)	2, 3, 4, 5, 6, 7	4.09 (*s*)	74.2 (*d*)
C(2)		121.2 (*s*)			121.5 (*s*)
C(3)		148.2 (*s*)			148.0 (*s*)
C(4)		112.4 (*s*)			112.9 (*s*)
H–C(5)	6.35 (*s*)	131.2 (*d*)	2, 3, 4	6.42 (*s*)	131.0 (*d*)
C(6)		91.5 (*s*)			91.0 (*s*)
H_a–C(7)	3.05 (*d*, J=18.5)	39.1 (*t*)	1, 6, 8	3.10 (*d*, J=18.4)	37.9 (*t*)
H_b–C(7)	3.94 (*d*, J=18.5)			3.79 (*d*, J=18.4)	
C(8)		154.3 (*s*)			154.0 (*s*)
C(9)		159.0 (*s*)			160.3 (*s*)
CH_2(10)	3.70 (*td*, J=6.0)	37.2 (*t*)	9, 11, 12	3.59 (*t*, J=7.2)	36.7 (*t*)
CH_2(11)	2.13 (*tt*, J=6.0)	29.3 (*t*)	10, 12	2.12 (*tt*, J=6.6)	29.3 (*t*)
CH_2(12)	4.10 (*t*, J=5.7)	91.2 (*t*)	4, 10	4.07 (*t*, J=6.0)	70.9 (*t*)
C(13)		151.5 (*s*)			152.1 (*s*)
C(14, 18)		118.3 (*s*)			118.1 (*s*)
H–C(15, 17)	7.37 (*s*)	133.0 (*d*)	13, 14/18	7.52 (*s*)	133.0 (*d*)
C(16)		137.6 (*s*)			136.7 (*s*)
CH_2(19)	2.80 (*t*, J=6.9)	34.4 (*t*)	16	2.85 (*t*, J=7.2)	33.1 (*t*)
CH_2(20)	3.56 (*td*, J=6.9)	38.9 (*t*)	15/17, 16, 19, 21	3.09 (*t*, J=6.6)	40.7 (*t*)
H–C(21)	8.19 (*s*)	161.4 (*d*)		8.55 (*s*)	169.1 (*d*)
MeO	3.74 (*s*)	60.2 (*q*)	3	3.73 (*s*)	59.2 (*q*)
H–N–C(9)	7.16 (br. *t*)				
H–N–C(20)	5.60 (br. *t*)				

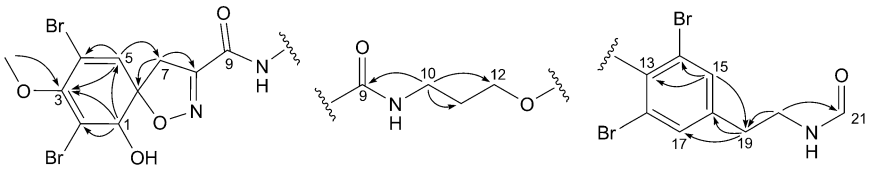

Fig. 3. *Substructures and diagnostic HMBCs*

2.80 (CH_2(19)), 3.56 (CH_2(20)), 5.60 (H–N–C(20)) in the ^{1}H,^{1}H-COSY spectrum, and the HMBC of δ(H) 3.56 (CH_2(20)) to the signal of the aldehyde C-atom C(21) (δ(C) 161.4). The HMBC of δ(H) 2.80 to the signals of C(16) (δ(C) 137.6) and C(15, 17) (δ(C) 133.0), and additionally between the signals of the aryl H-atom (δ(H) 7.37) to those of C(13) (δ(C) 151.5), C(14, 18) (δ(C) 118.3), and C(16) (δ(C) 137.6) connected the aryl moiety to the ethylformamide moiety as shown in substructure **C** (*Fig. 3*), thus completing the structure of compound **2**.

The *trans*-configuration of the vicinal O-atoms at C(1) and C(6) was established based on the chemical shifts of H–C(1), H_a–C(7), and H_b–C(7), and it is consistent

with the relative configuration of all reported natural spiro[cyclohexadien-isoxazole] compounds: the *cis*-isomer, which exhibited a broad *singlet* for both H_a–C(7) and H_b–C(7) has only been reported from chemical synthesis [27]. A negative optical rotation $[\alpha]_D = -72$ and negative *Cotton* effects at 248 and 285 nm in the CD spectrum indicated a (1*S*,6*R*) absolute configuration for the dibromo-spiro[cyclohexadien-isoxazole] moiety, consistent with related spiroisoxazole compounds [28], the absolute configuration of which have been established by X-ray crystallography and CD analysis.

The structure of compound **2** has been confirmed by semi-synthesis. Formylation of araplysillin I (**1**) furnished a semi-synthetic product with NMR spectra identical to the natural product.

Compound **3** was obtained as an optically active oily solid ($[\alpha]_D^{25} = -69$, $c = 0.02$, MeOH). The LR-ESI-MS spectrum (negative-ion mode) displayed two 1:3:5:3:1 clusters of peaks centered at *m*/*z* 716 (parent peak) and 762 characteristic of a tetrabrominated compound. An accurate mass could not be obtained, but the peak at *m*/*z* 716 consistent with araplysillin I was repeatedly obtained. The IR and UV spectra of compound **3** were similar to compound **2**. The ^{13}C-NMR spectra (see *Table 2*) also revealed exactly the same types of C-atoms as compound **2**; these exhibit the same HMBCs, except for the aldehyde C-atom (δ(C) 169.1, *d*), which showed no HMBC. The two compounds, however, had very different solubilities: compound **2** was soluble in CH_2Cl_2, in contrast to compound **3**, which was only sparingly soluble. This suggested a difference between the two compounds in the terminal aldehyde moiety.

On the basis of the H- and C-atom chemical shifts, the terminal aldehyde C-atom is proposed to be either the formate salt of araplysillin I ($R–NH_3^+OCHO^-$), or the N-hydroxyformamide (N(OH)CHO). The formate salt of araplysillin I, prepared by treating the natural product **1** with two equivalents of HCOOH for one hour, was analyzed by ^{1}H-NMR spectroscopy in (D_6)DMSO and CD_3OD (see *Table 3*).

Table 3. *Comparison of ^{1}H-NMR* (300 MHz) *Spectroscopic Data of Compound* **3** *to the Formate Salt of Araplysillin I* (**1**)

Position	δ(H) in (D_6)DMSO			δ(H) in CD_3OD		
	Compound **3**	Formate salt	$\Delta\delta$(H)	Compound **3**	Formate salt	$\Delta\delta$(H)
H–C(15,17)	7.58	7.57	−0.01			
CH_2(19)	2.81	2.77	−0.04	2.85	2.90	+0.05
CH_2(20)	3.03	2.96	−0.07	3.09	3.17	+0.08
H–C(21)	8.26	8.37	+0.11	8.55	8.21	−0.34

The signals for the H-atoms H–C(1) to CH_2(12) for the natural product **3** and for the formate salt of **1** were identical in both solvents, but differences were observed for the signals of H–C(15,17) and particularly CH_2(19), CH_2(20), and H–C(21); these differences (for example $\Delta\delta$(H) 0.34 ppm for the aldehyde H-atom H–C(21) in CD_3OD) showed clearly that compound **3** cannot be the formate salt. Furthermore, the (D_6)DMSO ^{1}H-NMR spectrum of the natural product **3** revealed only one amide H-atom, H–N–C(9) which supported the presence of a *N*-hydroxyformamide. The

molecular formula $C_{22}H_{23}Br_4N_3O_7$ and structure **3** were, therefore, proposed for this compound.

Compounds **5**, **6**, and **7** were isolated from the araplysillin-containing sponge *I* and named araplysillins IV, V, and VI, respectively. Araplysillins IV (**5**) and V (**6**) were obtained as optically active amorphous solids, closely related to araplysillin II, and both differing from this compound by their alkyl chain, with respectively two and four additional CH_2 groups. Furthermore, the terminal group of the side chain was a Me instead of an ^{i}Pr group, and the alkyl chain bears a Me group.

The Me H-atom signals of the ^{1}H-NMR spectrum of araplysillin IV (**5**; *Table 4*) at δ(H) 0.86 (*d*, $J = 6.6$) and δ(H) 0.91 (*t*, $J = 6.6$) indicated a branched alkyl chain. HMBCs of the Me group signal at δ(H) 0.91 (Me(36)) to those of the C-atoms C(35) (δ(C) 22.7) and C(34) (δ(C) 32.0) established the alkyl chain terminus as $-CH_2CH_2$ Me.

HMBCs of the signal of Me(37) (δ(H) 0.86, *d*, $J = 6.6$) to those of the CH (δ(C) 32.8) and CH_2 (δ(C) 37.2) C-atoms suggested the partial structure $-CH_2CH(Me)CH_2-$. These HMBCs suggested also that the point of branching must be at least four C-atoms away from the alkyl terminus. Attempts to determine the point of methylation with electron impact mass spectrometry (EI-MS) proved unsuccessful. Therefore, the alkyl chain C-atoms were assigned on the basis of 2D-NMR experiments, comparisons to literature, and ChemDraw spectra simulation. HMBCs of the signal of CH_2(20) (δ(H) 3.49, *td*) to those of both C(16) (δ(C) 138.1), C(19) (δ(C) 34.5), and of the CO group C(21) (δ(C) 173.4), and further HMBCs between the signal of CH_2(22) (δ(H) 2.12–2.20, *m*) to those of C(21) (δ(C) 173.4), C(23) (δ(C) 25.8), and C(24) (δ(C) 29.4), established the connectivity of the amide to the alkyl chain, $Ar-CH_2CH_2NHCOCH_2CH_2-$. Connectivity between C(22), C(23), and C(24) was supported by the spin system δ(H) 2.12–2.20 (*m*), 1.58–1.63 (*m*), 1.21–1.34 (*m*) observed in the COSY spectrum, and it was identical to their counterparts for the known compound, araplysillin II (**4**). The branching point of the alkyl chain was deduced from comparisons to C-atom chemical shifts of glycolipids (see *Fig. 4*, substructure **D**) of the same length reported from another verongid sponge [29], whose branching positions have been unambiguously assigned by EI-MS. Besides C-atom chemical shifts identical to literature, the C-atoms around the branched Me group also reveal a certain symmetry in their chemical shifts; this symmetry is exploited by ChemDraw spectra simulation to identify changes enforced by different points of methylation on the chemical shifts of the motif of interest (as illustrated in with bold C–C bonds in *Fig. 4*, substructures **D**, **E**, and **F**). These simulations revealed that methylation after C-atom C(30) (*e.g.* at C(31) as in substructure **E**) or before C(28) (*e.g.* at C(27) as in substructure **F**) disturbs the chemical shift symmetry. The predicted point of methylation is consequently restricted to C-atoms C(28), C(29), or C(30). On this basis, and due to the very close correlation to literature, araplysillin IV (**5**) was assigned the terminal alkyl moiety **D**[1]).

Araplysillin V (**6**), isolated as a translucent, optically active solid ($[\alpha]_D^{25} = -50$, $c =$ 0.002, MeOH) and exhibited in the HR-DCI-MS-CH_4 (negative-ion mode) spectrum a 1:3:5:3:1 cluster of peaks centered at *m/z* 997.1082 (Δ −0.1 mmu) consistent with a

[1]) Notice the asymmetry in the predicted chemical shifts in the simulations **E** and **F**.

Table 4. *NMR Spectroscopic Data for Araplysillins IV* (**5**) *and V* (**6**). Measured in $CDCl_3$; ^{1}H-NMR spectra at 500 MHz; ^{13}C-NMR spectra at 125 MHz, resp.

Position	**5**			Position	**6**		
	δ(H)	δ(C)	HMBC		δ(H)	δ(C)	HMBC
H–C(1)	4.43 (br. *s*)	74.1 (*d*)	2, 6	H–C(1)	4.40 (br. *s*)	74.0	3, 5, 6, 9
C(2)		121.2 (*s*)		C(2)		121.2	
C(3)		148.2 (*s*)		C(3)		149.2	
C(4)		112.3 (*s*)		C(4)		112.5	
H–C(5)	6.36 (*s*)	131.2 (*d*)	1, 2, 4, 7	H–C(5)	6.34 (*s*)	131.2	1, 2, 3, 4, 7
C(6)		91.5 (*s*)		C(6)		91.4	
H_a–C(7)	3.06 (*d*, $J = 18.5$)	38.9 (*t*)	1, 5, 6, 8	H_a–C(7)	3.05 (*d*, $J = 18.5$)	38.9	1, 5, 6, 8
H_b–C(7)	3.99 (*d*, $J = 18.5$)			H_b–C(7)	3.98 (*d*, $J = 18.5$)		
C(8)		157.3 (*s*)		C(8)		154.3	
C(9)		159.0 (*s*)		C(9)		159.0	
CH_2(10)	3.73 (*td*, J=6.2)	37.2 (*t*)	9, 11, 12	CH_2(10)	3.72 (*td*, J=6.2)	37.2	9, 11, 12
CH_2(11)	2.13 (*tt*, J=6.0)	29.4 (*t*)		CH_2(11)	2.13 (*tt*, J=6.0)	29.4	
CH_2(12)	4.11 (*t*, J=5.8)	71.1 (*t*)	10	CH_2(12)	4.10 (*t*, J=5.8)	71.1	10, 11
C(13)		151.4 (*s*)		C(13)		151.3	
C(14,18)		118.2 (*s*)		C(14,18)		118.2	
H–C(15,17)	7.36 (*s*)	133.0 (*d*)	13, 14/18, 19	H–C(15,17)	7.35 (*s*)	133.0	13, 14/18, 19
C(16)		138.1 (*s*)		C(16)		138.1	
CH_2(19)	2.77 (*t*, J=6.9)	34.5 (*t*)	15/17, 16, 20	CH_2(19)	2.76 (*t*, J=7.0)	34.6	15/17, 16, 20
CH_2(20)	3.49 (*td*, J=6.7)	40.4 (*t*)	16, 19, 21	CH_2(20)	3.48 (*td*, J=7.0)	40.4	16, 19, 21
C(21)		173.4 (*s*)		C(21)		173.3	
CH_2(22)	2.12–2.20 (*m*)	36.9 (*t*)	21, 23, 24	CH_2(22)	2.13–2.20 (*m*)	36.9	23, 24
CH_2(23)	1.58–1.63 (*m*)	25.8 (*t*)	22	CH_2(23)	1.60–1.64 (*m*)	25.8	22
CH_2(24–27)	1.28–1.31 (*m*)	29.3–30.1 (*t*)		CH_2(24–29)	1.28–1.31 (*m*)	29.3–30.1	
CH_2(28)	1.28–1.31 (*m*)	27.1 (*t*)		CH_2(30)	1.28–1.31 (*m*)	27.1	
CH_2(29)	1.05–1.16 (*m*)	37.2 (*t*)		CH_2(31)	1.05–1.1 (*m*)	37.1	39
H–C(30)	1.21–1.34 (*m*)	32.8 (*d*)		H–C(32)	1.30–1.40 (*m*)	32.7	
CH_2(31)	1.21–1.34 (*m*)	37.2 (*t*)		CH_2(33)	1.28–1.31 (*m*)	37.1	
CH_2(32)	1.21–1.34 (*m*)	27.1 (*t*)		CH_2(34)	1.28–1.31 (*m*)	27.1	
CH_2(33)	1.21–1.31 (*m*)	29.3–30.1 (*t*)		CH_2(35)	1.28–1.31 (*m*)	29.3–30.1	
CH_2(34)	1.21–1.34 (*m*)	32.0 (*t*)		CH_2(36)	1.28–1.31 (*m*)	31.9	
CH_2(35)	1.27–1.31 (*m*)	22.7 (*t*)		CH_2(37)	1.28–1.31 (*m*)	22.7	
Me(36)	0.91 (*t*, J=6.6)	14.2 (*q*)		Me(38)	0.91 (*t*, J=6.6)	14.2	
Me(37)	0.86 (*d*, $J = 6.6$)	19.8 (*q*)	29/31, 30	Me(39)	0.85 (*d*)	19.7	31/33, 32
MeO	3.77 (*s*)	60.2 (*q*)	3	MeO	3.76 (*s*)	60.2	3
H–N–C(9)	7.17 (*t*, $J = 6.0$)			H–N–C(9)	7.17 (*t*, $J = 6.0$)		9
H–N–C(20)	5.48 (br. *t*, $J = 6.1$)			H–N–C(20)	5.48 (br. *t*, $J = 6.1$)		20, 21

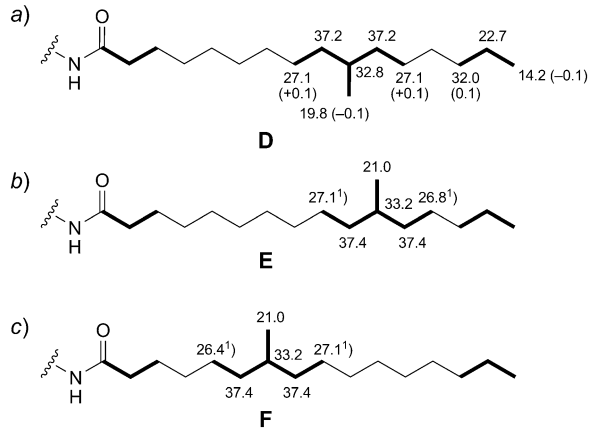

Fig. 4. *Superimposition of observed spectroscopic data on literature* (**D**) *for the terminal alkyl chain of araplysillin IV* (**5**) *and ChemDraw spectra simulation* (**E** and **F**). *a*) Observed chemical shifts and difference to literature (number in bracket) for methylation at C(30). *b*) ChemDraw-predicted chemical shifts for methylation at C(31). *c*) ChemDraw-predicted chemical shifts for methylation at C(27).

tetrabrominated compound. The mass suggested a molecular formula of $C_{40}H_{59}Br_4N_3O_6$, possessing eleven degrees of unsaturation. The UV, IR, 1D- and 2D-NMR data suggested that araplysillin V (**6**) is very similar to compound **5**, while the molecular mass indicated that the alkyl chain of compound **6** was two CH_2 units longer. The alkyl chain of compound **6** was characterized in the same manner as for compound **5**; the C-atoms were assigned from comparison to literature, HMBC, COSY, and ChemDraw spectra simulation. The point of branching was thus proposed to be at C(32).

Araplysillin VI (**7**) was obtained as an amorphous, optically inactive solid. It differed from araplysillin II only by its oxazolidine moiety, which lacked the spiro quaternary C-atom. The ^{1}H-NMR (*Table 5*) revealed *singlet*s at δ(H) 7.59 (1 H) and δ(H) 7.31 (2 H) to indicate two aryl moieties. The HMBC spectrum revealed that the aryl H-atom with the signal at δ(H) 7.59 was part of a ring-opened spiro-isoxazole-derived moiety (see *Fig. 5*, substructure **G**).

The HMBCs of the signal at δ(H) 7.59 (H–C(5)) to those of the C-atoms C(2) (δ(C) 108.5), C(3) (δ(C) 153.4), and C(4) (δ(C) 106.9), of the signal of MeO (δ(H) 3.86) to the signal of C(3) (δ(C) 153.4), and correlations of the signal of H–C(7) (δ(H) 3.86) to those of the C-atoms C(1) (δ(C) 154.0), C(6) (δ(C) 120.3), C(8) (δ(C) 150.5), and C(9)=O (δ(C) 165.0) supported the sub-structure **G** (*Fig. 5*). An additional HMBC of the signals of the OH group at δ(H) 10.27 to the signal of C(8) (δ(C) 150.5) supported an oxime moiety. The ^{1}H,^{1}H-COSY spectrum revealed the spin systems δ(H) 7.66 (H–N–C(9)), 3.70 (CH_2(10)), 2.06 (CH_2(11), 4.06 (CH_2(12)) for an *O*-propylamine moiety. The HMBC of the signal δ(H) 3.70 (CH_2(10)) to the one of C(9)= O (δ(C) 165.0) established the connectivity of the *O*-propylamine group to substructure **G** as for araplysillin II (**4**).

Table 5. *NMR Spectroscopic Data for Araplysillin VI* (**7**; measured in $CDCl_3$; at 500 MHz for ^{1}H- and 125 MHz for ^{13}C-NMR)

Position	δ(H)	δ(C)	COSY	HMBC
C(1)		154.0 (*s*)		
C(2)		108.5 (*s*)		
C(3)		153.4 (*s*)		
C(4)		106.9 (*s*)		
H–C(5)	7.59 (*s*)	134.2 (*d*)		1, 2, 3, 4, 7
C(6)		120.3 (*s*)		
CH_2(7)	3.86 (*s*)	24.8 (*t*)		1, 6, 8, 9
C(8)		150.5 (*s*)		
C(9)		165.0 (*s*)		
CH_2(10)	3.70 (*td*, *J* = 6.0)	37.7 (*t*)	NH-9	9, 11, 12
CH_2(11)	2.06 (*tt*, *J* = 5.8)	28.9 (*t*)	10, 12	
CH_2(12)	4.06 (*t*, *J* = 5.5)	71.4 (*t*)		
C(13)		151.3 (*s*)		
C(14, 18)		118.0 (*s*)		
C(15, 17)	7.31 (*s*)	133.0 (*d*)		13, 15/17, 14/18, 19
C(16)		137.9 (*s*)		
CH_2(19)	2.73 (*t*, *J* = 6.8)	34.8 (*t*)		16, 15/17
CH_2(20)	3.47 (*q*, *J* = 6.3)	40.4 (*t*)	19, NH-20	19, 21
C(21)		174.2 (*s*)		
CH_2(22)	2.17 (*t*, *J* = 7.5)	36.9 (*t*)		21, 23, 24
CH_2(23)	1.56–1.64 (*m*)	25.9 (*t*)	22, 2	24
CH_2(24–30)	1.26–1.29 (*m*)	29.3–29.8 (*t*)		
CH_2(31)	1.20–1.31 (*m*)	27.5 (*t*)		
CH_2(32)	1.10–1.17 (*m*)	39.1 (*t*)		
C(33)	1.47–1.61 (*m*)	28.0 (*s*)	32, 34/35	34/35
Me(34, 35)	0.88 (*d*, *J* = 6.5)	22.7 (*q*)		31, 32
MeO	3.86 (*s*)	60.5 (*q*)		3
HO–N	10.27 (br. *s*)		8	
H–N–C(9)	7.66 (br. *t*, *J* = 6.0)			
H–N–C(20)	5.81 (br. *s*)			

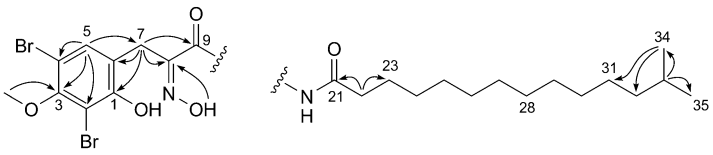

Fig. 5. *Key HMBC for substructures* **G** *and* **H** *of araplysillin VI* (**7**)

Compounds **1**–**3**, **5**, and **6** were assigned the same configuration on the basis of their negative optical rotation values and their negative *Cotton* effects at 248 and 285 nm in the CD spectrum similar to the data for (–)-aerothionin [27][28].

2. *Biological Studies.* In the aim of finding more specific antimalarial compounds, all isolated compounds were tested on protein farnesyl transferase (= PFTase), *Plasmo-*

dium falciparum, and for cytotoxicity. Antiplasmodial and PFTase activity in these *Suberea* compounds were associated with brominated compounds (*Table 6*).

Table 6. *Biological Activities of Compounds Isolated from* S. ianthelliformis *Sponge Samples*

	IC_{50} [μM]				Inhibition [%]	Selectivity Index (*SI*)[a])
	MCF-7[b])	Vero[c])	FcB-1[d])	3D7[e])	PFTase (10 μg/ml)	
Aureole	14.3	10.8	NA[f])	NA	180[g])	–[h])
Aplysterol	NA	–	NA	–	11	
Araplysillin I (**1**)	7.2	25.3	4.5	4.6	32	5.6
Araplysillin I (**1**) salt	14.0	29.4	5.3	4.5	27	5.5
Araplysillin N20-formamide (**2**)	3.8	5.0	3.6	7.0	28	1.4
Araplysillin N20-hydroxyformamide (**3**)	–	–	5.0	4.1	21	–
Araplysillin II (**4**)[i])	–	107	34.2	–	23	3.0
Araplysillin IV (**5**)[j])	–	–	27.6	–	21	–
Araplysillin V (**6**)	–	–	50.5	–	17	–
Araplysillin VI (**7**)	–	–	37.4	–	120[g])	–
Aerophobin I (**8**)	–	–	59.0	–	37	–
Aerophobin II (**9**)	–	19.9	24.9	19.9	64	0.8
Purealidin Q (**10**)	–	–	3.6	–	11	–
Aerothionin (**11**)	4.6	4.8	3.4	4.2	38	1.4
Homoaerothionin (**12**)	4.9	9.0	2.8	4.0	28	3.2
Aplysinone D (**13**)	0.6	3.6	1.0	3.1	–	3.6
11,19-Dideoxyfistularin 3 (**14**)	0.8	0.5	2.1	0.9	38	0.2
11-Hydroxyfistularin 3 (**15**)	2.0	3.2	2.1	2.6	46	1.5
Chloroquine diphosphate[i])	–	–	0.145	0.072		
Doxorubicin[j])	0.5	0.3	–	–		

[a]) *SI* calculated for FCB-1/Vero inhibitions. [b]) MCF-7: Michigan Center Foundation-7 breast cancer cell line. [c]) Vero: Vero cell line. [d]) FcB-1: chloroquine-resistant strain of *P. falciparum*. [e]) 3D7: chloroquine-sensitive strain of *P. falciparum*. [f]) NA: inactive at 32 μM (aureole) and 24 μM (aplysterol). [g]) % PFTase activation. [h]) –, not tested. [i]) Positive control for the antiplasmodial tests. [j]) Positive control for the cytotoxity bioassays.

All bromotyrosine compounds tested exhibited moderate to weak inhibitory activities against chloroquine-resistant and -sensitive *P. falciparum* strains, FcB-1 and 3D7, with IC_{50} values in the range of 1.0 to 59 μM and 0.9 to 19.9 μM, respectively. Antiplasmodial activity was in the same range on both strains. Most compounds however showed minimal selective antiplasmodial activity. Among those compounds, araplysillin I (**1**) exhibited the best selectivity (though not the most potent activity) toward *P. falciparum*, with a selectivity index of 5.5 (calculated for Vero cells). Analogues of araplysillin I containing long terminal aliphatic chains, such as araplysillins II (**2**), IV (**5**), and V (**6**), were seven times less active against the *P. falciparum* strain FcB-1. Similarly, the presence of an imidazole ring lowered significantly antiplasmodial activity. On the other hand, araplysillin N(20)-formamide (**2**) exhibited similar antiplasmodial activity though elevated cytotoxicities against MCF-7 and Vero cells, which gave a poor antiplasmodial selectivity.

Dimeric dibromospirocyclohexadienylisoxazoline compounds, such as 11,19-dideoxyfistularin 3 (**14**) and 11-hydroxyfistularin 3 (**15**) exhibited greater toxicities against *P. falciparum* ($IC_{50}=0.9$ μM), but also against MCF-7 and Vero cells. Demethoxylation (*e.g.*, aplysinone D (**13**)) of the 3,5-dibromo-4-methoxycyclohexa-2,4-dienol moiety did not alter its toxicity to either *P. falciparum*, MCF-7, or Vero cells.

All compounds with the 3,5-dibromo-1-hydroxy-4-methoxycyclohexadienyl isoxazoline motiety (**1**–**6**, **8**–**12**) and their demethoxylated analogues (**13**–**15**) exhibited mild inhibitory activity against human PFTase. All these compounds inhibited the enzyme at 11–68% inhibition at 10 μg/ml. A notable exception, compound **7**, activated the farnesylation, in contrast to the other dibrominated metabolites. The loss of the isoxazole moiety and the subsequent aromatization of the 3,5-dibromo-1-hydroxy-4-methoxycyclohexadienyl part of the molecule is likely to be responsible for the difference in PFTase inhibitory activity. The only other metabolite possessing PFTase activation properties, the terpene aureole, is inactive against *P. falciparum*. The PFTase inhibitory activity of these compounds is not linked to the toxicity on *P. falciparum*, as the best PFTase inhibitor, araplysillin V (**6**), is only weakly antiplasmodial. It shows how difficult it is to give a conclusion from *in vitro* to *in cellulo* bioassay on mildly active compounds.

3. *Chemotaxonomy.* Chemotaxonomy was compared against genomic data. For the four target specimens, DNA fragments of 644–657 nucleotides of a fragment of the nuclear ribosomal cistron (5.8S rDNA partial, ITS-2, and 28S rDNA partial) have been received, resulting in a data set of 670 characters. This fragment possesses a conservative part (the 28S region), which is necessary to verify that the fragment derives from the sponge and not of the numerous sponge associates. In contrast, its ITS-2 region is sufficiently variable to display inter- and intraspecific differences. An unambiguous alignment for all four species and over all positions has not been possible because the sequences fell into two different sequence signatures, which comprised Samples *I*+*II* and *III*+*IV*, respectively (*Fig. 6*).

Samples *I* and *II* share a 99% nucleotide identity for the sequenced fragment, which corroborates their biochemical properties. Sponges *I* and *II* produce only monomeric spirooxazolin compounds and share close structures related to araplysillin. Such high sequence similarity, particularly in a fast evolving fragment such as ITS-2, might indicate that both specimens are conspecific – however such a genetic species concept is yet not applicable for sponges. Sponges *III* and *IV* are different; both share only 93% of the genetic character positions and possess more significant chemical differences. Sample *III* produces dimeric spirooxazolines, and sample *IV* did not reveal any bromotyrosine-derived compounds. These differences are likewise in congruence with our molecular genetics findings.

This work is part of the Ph.D. thesis of *L. M.* thesis supported by *IRD* and *CRISP* (*Coral Reef Initiative in the South Pacific*) that we acknowledge here. This work was run within the C2 component of the *CRISP* project, granted by the *Agence Française de Développement* and *IRD*. We thank the Solomon Islands Government for permission to collect the specimens, the Fisheries Department and *R. Sulu* (University of the South Pacific in Honiara) for their on-field assistance. We also thank *C. Zedde* (responsible for HPLC facilities in UMR 5068 CNRS-Université Toulouse 3) for her assistance.

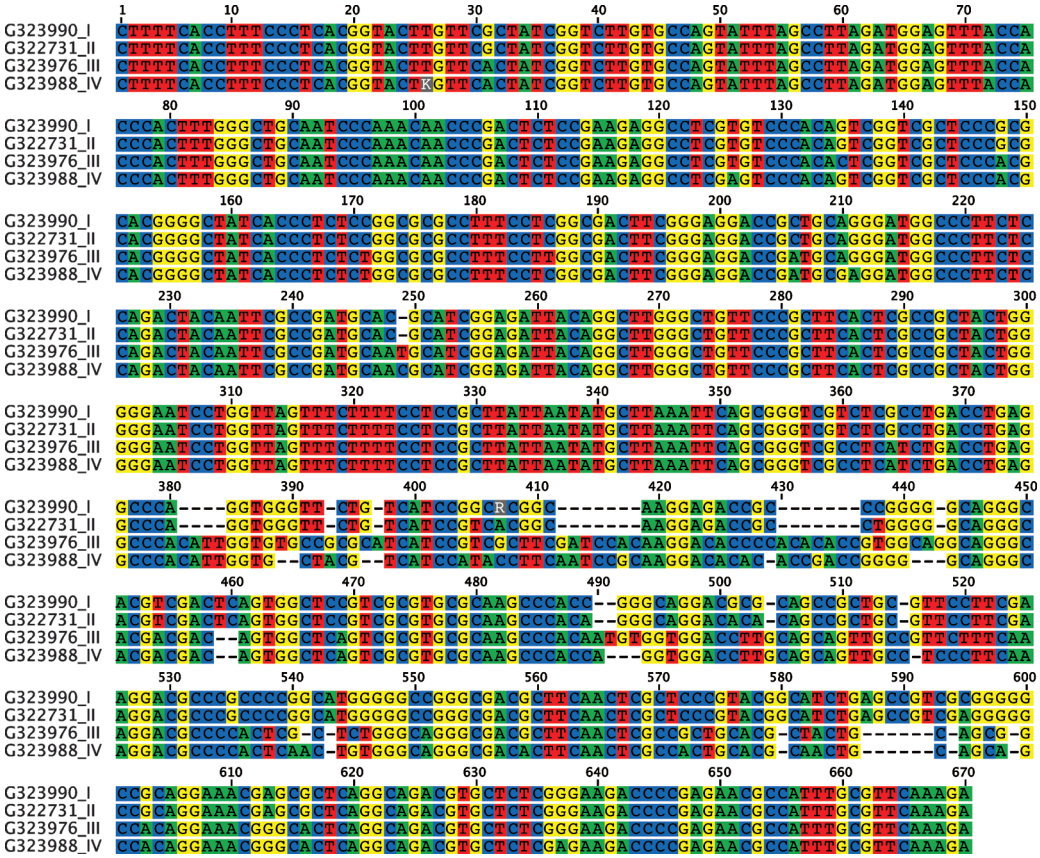

Fig. 6. *The 28S-ITS-2 rDNA data set for the four specimens investigated*

Experimental Part

General. Flash column chromatography (FCC): silica gel (SiO_2, 40–63 μm; *Interchrom*) with solvents (cyclohexane, $CHCl_3$, CH_2Cl_2, AcOEt, and MeOH) of HPLC-grade. H_2O used for RP-HPLC was distilled and filtered *via* 0.2-μm nylon filters. Analytical and preparative HPLC: *Waters* LC/MS system equipped with a *Waters 2545* binary gradient module, *29998* photodiode array detector and a *3100* mass detector using *XBridge C18* columns (4.6 mm × 180 mm; 19 mm × 150 mm; ∅ 5 μm). Optical rotations: *Perkin-Elmer 241* polarimeter. IR Spectra: *Perkin-Elmer Paragon 1000* FT-IR spectrometer. Circular dichroism spectra: *JASCO-J-815 CD* spectrometer using 300-μl *Helma-semi Micro* absorption cuvettes. 1D- and 2D-NMR spectra : *Bruker Avance 300* and *500* MHz spectrometers, with chemical shifts referenced for the residual solvent signals for $CDCl_3$ (δ(H) 7.28 and δ(C) 77.0) and CD_3OD (δ(H) 3.31 and δ(C) 47.7). MS: *Finnigan LCQ DECA XP MAS* (*Thermo-Electron Corp.*) mass spectrometer. HR-ESI-MS: *Waters LCT TOF* mass spectrometer with data acquired and processed with the MassLynx NT software system. HR-DCI-MS-CH_4 spectra: *GCT Premier CAB109* orthogonal acceleration time-of-flight (oa-TOF) mass spectrometer. Radioactivity was measured on a *1450-Microbeta* trilux, *Wallac Perkin-Elmer* β-counter.

Biological Material. The four *Suberea ianthelliformis* sponges were collected in July 2004 using SCUBA from the following locations: Anuta Paina Island (Malaita) (sponge *I*, 30 m deep), New Georgia Island (sponge *II*, 20 m), North West of Nggela Island (sponge *III*, 18 m), and Three Sisters Island

(sponge *IV*, 20 m). Voucher specimens of sponges *I*–*IV* are deposited with the Queensland Museum (Brisbane, Australia) under the access Nos. G323990, G322731, G323976, and G323988, resp.

Extraction and Isolation. The freeze-dried sponges (208 g, 59 g, and 206 g resp., for sponges *I*, *II*, and *III*) were exhaustively extracted with EtOH/H_2O 80:20, followed by extraction with 98% EtOH. The alcoholic extracts were evaporated and then partitioned between CH_2Cl_2 and H_2O/MeOH to furnish an org. and a H_2O/MeOH fraction. The H_2O/MeOH fractions were 1.2 g, 1.0 g, and 1.5 g, and the org. fractions were 5.3 g, 1.05 g, and 17.3 g, for sponges *I*, *II*, and *III*, resp. Twelve known and five new compounds were isolated and identified. *Araplysillin N20-formamide* (**2**; 3.1 mg) was obtained from the org. fraction of sponge *I* (4.7 g) by successive SiO_2 CC eluted with cyclohexane/AcOEt and CH_2Cl_2/MeOH mixtures, followed by size-exclusion chromatography (*Sephadex LH-20*, CH_2Cl_2). *Araplysillin N20-hydroxyformamide* (**3**; 3.1 mg) was obtained from the H_2O/MeOH fraction of sponge *II*. Trituration of this extract (1.2 g) with CH_2Cl_2/MeOH 6:4 followed by size-exclusion chromatography (*LH-20*, CH_2Cl_2/MeOH 6:4) and successive SiO_2 CC eluted with mixtures of CH_2Cl_2/MeOH/NH_4^+ furnished compound **3**. *Araplysillins IV* (**5**; 3 mg), *V* (**6**; 2.3 mg), and *VI* (**7**; 2.2 mg) were obtained pure from sponge *I* after further purification of the apolar fractions of the above fractionation using SiO_2 CC eluted with CH_2Cl_2/MeOH mixtures, followed by RP-HPLC (MeOH/H_2O 85:15 to 90:10).

Araplysillin N20-Formamide (=*(5S,10R)-7,9-Dibromo*-N-*(3-{2,6-dibromo-4-[2-(formylamino)-ethyl]phenoxy}propyl)-10-hydroxy-8-methoxy-1-oxa-2-azaspiro[4.5]deca-2,6,8-triene-3-carboxamide*; **2**). Amorphous solid. $[\alpha]_D^{25} = -72$ ($c = 0.01$, MeOH). UV (MeOH): 220 (4.18), 285 (1.05). CD (MeOH): 248 (−7.5), 285 (−7.0). IR (CH_2Cl_2): 3307, 3060, 2934, 1733, 1659, 1534, 1259, 1046, 735. ^{1}H- and ^{13}C-NMR: see *Table 2*. LR-ESI-MS: 764.15 (22, $[M+Na]^+$), 766.18 (66), 768.10 (100), 770.06 (67), 773.06 (24). HR-DCI-MS-CH_4: 763.8254 (20, $[M+Na]^+$), 765.8213 (66), 767.8170 (100), 769.8198 (64), 771.8236 (18), 741.8404 (20, $[M+H]^+$), 743.8355 (66), 743.8318 (100), 747.8348 (64), 749.8 (6).

Semi-Synthesis of Compound **2**. A 1.5 ml-aliquot of a 1:5 Ac_2O/HCO_2H mixture was sparingly added to 50 mg of **1** dissolved in 1 ml pyridine. After the reaction was complete (less than 1 h), H_2O was added, alkalinized with NH_4OH, then extracted with CH_2Cl_2. After drying ($MgSO_4$), the product was dried *in vacuo* and subjected to purification *via* SiO_2 CC with a CH_2Cl_2/MeOH 98.5:1.5 solvent system. ^{1}H-NMR and chromatographic data were identical to those of the natural product **2**.

Araplysillin N20-Hydroxyformamide (=*(5S,10R)-7,9-Dibromo*-N-*[3-(2,6-dibromo-4-{2-[formyl-(hydroxy)amino]ethyl}phenoxy)propyl]-10-hydroxy-8-methoxy-1-oxa-2-azaspiro[4.5]deca-2,6,8-triene-3-carboxamide*; **3**). Amorphous solid. $[\alpha]_D^{25} = -69$ ($c = 0.02$, MeOH). UV (MeOH): 220 (4.06), 285 (9.2). CD (MeOH): 248 (−13.8), 285 (−12.8). IR (MeOH): 3349, 3053, 2926, 1658, 1589, 1531, 1452, 1378, 1252, 1046, 734. ^{1}H- and ^{13}C-NMR: see *Table 2*. LR-ESI-MS: 757.86 (20, $[M+H]^+$), 759.80 (66), 761.81 (100), 763.80 (66), 765.8 (20), 716 (100).

Araplysillin IV (=*(5S,10R)-7,9-Dibromo*-N-*[3-(2,6-dibromo-4-{2-[(10-methylhexadecanoyl)amino]ethyl}phenoxy)propyl]-10-hydroxy-8-methoxy-1-oxa-2-azaspiro[4.5]deca-2,6,8-triene-3-carboxamide*; **5**). Amorphous solid. $[\alpha]_D^{25} = -60$ (*c* 0.002, MeOH). UV (MeOH): 209 (1.06), 220 (sh, 4.10), 285 (1.20). CD (MeOH): 248 (−8.3), 285 (−8.5). IR (CH_2Cl_2): 3300, 3071, 2912, 2849, 1655, 1598, 1539, 1455, 1254, 1049, 732. ^{1}H- and ^{13}C-NMR: see *Table 4*. ESI-MS: 1016.3 (20, $[M+Na]^+$), 1018.3 (65), 1020.3 (100), 1022.3 (70), 1024.3 (20). HR-DCI-MS-CH_4: 965.0778 (10), 967.0787 (60), 969.0774 (100, M^-, $C_{38}H_{55}Br_4N_3O_6^-$; calc. 969.0779), 971.0768 (65), 973.0820 (20).

Araplysillin V (=*(5S,10R)-7,9-Dibromo*-N-*[3-(2,6-dibromo-4-{2-[(12-methyloctadecanoyl)amino]ethyl}phenoxy)propyl]-10-hydroxy-8-methoxy-1-oxa-2-azaspiro[4.5]deca-2,6,8-triene-3-carboxamide*; **6**). Amorphous solid. $[\alpha]_D^{25} = -50$ ($c = 0.002$, MeOH). CD (MeOH): 248 (−11.5), 285 (−10.5). IR (CH_2Cl_2): 3309, 2918, 2856, 1647, 1597, 1539, 1456, 1255, 735. ^{1}H- and ^{13}C-NMR: see *Table 4*. HR-DCI-MS-CH_4: 997.1082 (M^-, $C_{40}H_{59}Br_4N_3O_6^-$; calc. 997.1083). HR-DCI-MS-CH_4: 993.1137 (18), 995.1119 (66), 997.1103 (100, M^-), 999.1089 (70), 771.8236 (22).

Araplysillin VI (=N-*{2-[3,5-Dibromo-4-(3-{[3-(3,5-dibromo-2-hydroxy-4-methoxyphenyl)-2-(hydroxyimino)propanoyl]amino}propoxy)phenyl]ethyl}-13-methyltetradecanamide*; **7**). Amorphous solid. UV (MeOH): 232 (8.43), 286 (3.56). ^{1}H- and ^{13}C-NMR: see *Table 5*. HR-DCI-MS-CH_4: 937.0531 (10, M^-), 939.0571 (60), 941.0535 (100, M^-, $C_{36}H_{51}Br_4N_3O_6^-$; calc. 941.0532), 943.0536 (65), 945.0637 (20).

In vitro *Antiplasmodial Assays.* Antiplasmodial activity was evaluated by a radioactive micromethod [30]. The *Plasmodium falciparum* strains FCB1 and 3D7 (chloroquine-resistant and -sensitive

strains, resp.) were continuously cultured [31][32], and parasite cultures synchronized by lysis in 5% D-sorbitol [33]. The products were incubated in triplicate on 96-well plates containing parasite cultures (1.5% parasitemia +1.5% hematocrit) over 24 h at 37° over 5% CO_2. [^{3}H]Hypoxanthine was added to the product-parasite mixture, which was further incubated for 24 h, and then, parasitic growth was stopped by freezing. After defrosting, parasitic growth inhibition was evaluated by estimating [^{3}H]hypoxanthine incorporation and IC_{50} graphically determined in concentration *vs.* percent inhibition curves. Parasite cultures free of extracts were referred to as 100% growth and chloroquine-spiked cultures taken as positive controls.

Cytotoxicity Bioassays. Breast cancer cells MCF-7 and Vero cells were used to estimate cytotoxicity. Cells were cultured in conditions identical to parasite cultures, except for the replacement of 5% human serum with 5% fetal calf serum in the MCF-7 and Vero cells. Cell growth inhibition was determined, as for *P. falciparum*, by measuring [^{3}H]hypoxanthine incorporation. Doxorubicin was used as a positive control.

PFTase Bioassay. Extracts and pure compounds were screened in 96-well plates against human PFTase, and inhibitory activity was read on a *Wallac Victor* fluorimeter [34–36]. Assays were realized on 96-well plates, prepared with *Biomek NKMC* and *Biomek 3000* from *Beckman Coulter* and read on a *Wallac Victor* fluorimeter from *Perkin–Elmer*. In each well, 20 µl of farnesyl pyrophosphate (10 µM) was added to 180 µl of a soln. containing 2 µl of varied concentrations of potential inhibitors (dissolved in DMSO) and 178 µl of a soln. composed by 0.1 ml of partially purified recombinant human PFTase (1.5 mg/ml) and 7.0 ml of 2.5 µM Dansyl-GCVLS peptide (in the following buffer: 5.8 mM DTT, 6 mM $MgCl_2$, 12 µM $ZnCl_2$, 6 mM octyl D-glucopyranoside, and 53 mM *Tris*·HCl, pH 7.5). Then, the fluorescence development was recorded for 15 min (0.7 seconds per well, 20 repeats) at 30° with an excitation filter at 340 nm and an emission filter at 486 nm. Each measurement was realized as duplicate or triplicate.

Molecular Analyses. DNA was extracted using spin columns (*Qiagen*) following the manufacturer's protocol. ITS2 Fragments were amplified using the primers ITS-RA2 (GTC CCT GCC CTT TGT ACA CA) with ITS2.2 (CCT GGT TAG TTT CTT TTC CTC CGC) [37], or alternatively 5.8S-1-fwd (GTC GAT GAA GAA CGC AGC) with 28S-D2-rev (TCC GTG TTT CAA GAC GGG) [38]. Fragments were amplified under the following temp. regime: 94° 2 min, 35 cycles: 94° 30 s; 45° 20 s; 65° 60 s, followed by 72° 10 min. PCRs contained 11.25 µl ddH_2O, 4.15 µl dNTP (10 mM), 3.25 µl $MgCl_2$ (25 mM), 2.5 µl 10× *HotMaster* PCR Buffer, 2.5 µl BSA (100 mM, *Sigma*), 0.5 µl primer (10 mM), and 4 µl *HotMaster* polymerase (*Eppendorf*). Successful amplifications were sequenced on an *ABI 3730* capillary sequencer. Forward and reverse strands were base-called, clipped, and assembled using CodonCode Aligner v 2.0.4. The poriferan origin of the sequences was checked by a BLAST search [39] against the NCBI Genbank collection (http://www.ncbi.nlm.nih.gov/). MacClade v.4.08 [40] was used for pairwise alignments and Geneious 5.4 [41] for the statistics of genotype differences in the data set. Sequences are deposited with NCBI Genbank under accession numbers JN786373 (sponge *I*), JN786374 (sponge *II*), JN786375 (sponge *III*), and JN786376 (sponge *IV*).

REFERENCES

[1] A. M. S. Mayer, K. B. Glaser, C. Cuevas, R. S. Jacobs, W. Kem, R. D. Little, J. M. McIntosh, D. J. Newman, B. C. Potts, D. E. Shuster, *Trends Pharmacol. Sci.* **2010**, *31*, 255.
[2] J. M. Kornprobst, 'Encyclopedia of marine natural products', Wiley & Blackwell, New York, 2010.
[3] J. W. Blunt, B. R. Copp, M. H. G. Munro, P. T. Northcote, M. R. Prinsep, *Nat. Prod. Rep.* **2010**, *27*, 165.
[4] J. Pöppe, P. Sutcliffe, J. N. A. Hooper, G. Wörheide, D. Erpenbeck, *PLoS ONE* **2010**, *5*, e9950.
[5] D. Erpenbeck, R. W. M. Soest, *Mar. Biotechnol*. **2007**, *9*, 2.
[6] A. Al Mourabit, P. Potier, *Eur. J. Org. Chem.* **2001**, 237.
[7] L. Rahbœk, C. Christophersen, 'The Alkaloids: Chemistry and Biology', Vol. 57, Academic Press, 2001, p. 185.
[8] A. E. Wright, *Curr. Opin. Biotechnol.* **2010**, *21*, 801.

[9] C. Vergne, J. Appenzeller, C. Ratinaud, M.-T. Martin, C. Debitus, A. Zaparucha, A. Al-Mourabit, *Org. Lett.* **2008**, *10*, 493.
[10] D. Laurent, F. Pietra, *Mar. Biotechnol.* **2006**, *8*, 433.
[11] K. R. Watts, K.Tenney, P. Crews, *Curr. Opin. Biotechnol.* **2010**, *21*, 808.
[12] M. Gutiérrez, T. L. Capson, H. M. Guzmán, J. González, E. Ortega-Barría, E. Quiñoá, R. Riguera, *Pharm. Biol*. **2005**, *43*, 762.
[13] N. Lebouvier, V. Jullian, I. Desvignes, S. Maurel, A. Parenty, D. Dorin-Semblat, C. Doerig, M. Sauvain, D. Laurent, *Mar. Drugs* **2009**, *7*, 640.
[14] D. Chakrabarti, T. Da Silva, J. Barger, S. Paquette, H. Patel, S. Patterson, C. M. Allen, *J. Biol. Chem.* **2002**, *277*, 42066.
[15] R. T. Eastman, F. S. Buckner, K. Yokoyama, M. H. Gelb, W. C. Van Voorhis, *J. Lipid Res.* **2006**, *47*, 233.
[16] M. H. Gelb, W. C. Van Voorhis, F. S. Buckner, K. Yokoyama, R. Eastman, E. P. Carpenter, C. Panethymitaki, K. A. Brown, D. F. Smith, *Mol. Biochem. Parasitol.* **2003**, *126*, 155.
[17] L. Nallan, K. D. Bauer, P. Bendale, K. Rivas, K. Yokoyama, C. P. Hornéy, P. R. Pendyala, D. Floyd, L. J. Lombardo, D. K. Williams, A. Hamilton, S. Sebti, W. T. Windsor, P. C. Weber, F. S. Buckner, D. Chakrabarti, M. H. Gelb, W. C. Van Voorhis, *J. Med. Chem.* **2005**, *48*, 3704.
[18] J. Ohkanda, J. W. Lockman, K. Yokoyama, M. H. Gelb, S. L. Croft, H. Kendrick, M. I. Harrell, J. E. Feagin, M. A. Blaskovich, S. M. Sebti, A. D. Hamilton, *Bioorg. Med. Chem. Lett.* **2001**, *11*, 761.
[19] P. Djura, D. B. Stierle, B. Sullivan, D. J. Faulkner, E. V. Arnold, J. Clardy, *J. Org. Chem.* **1980**, *45*, 1435.
[20] P. De Luca, M. De Rosa, L. Minale, R. Puliti, G. Sodano, F. Giordano, L. Mazzarella, *J. Chem. Soc., Chem. Commun.* **1973**, 825.
[21] A. Longeon, M. Guyot, J. Vacelet, *Experientia* **1990**, *46*, 548.
[22] M. Gunasekera, S. P. Gunasekera, *J. Nat. Prod.* **1989**, *52*, 753.
[23] P. Ciminiello, E. Fattorusso, M. Forino, S. Magno, M. Pansini, *Tetrahedron* **1997**, *53*, 6565.
[24] C. J. Hernández-Guerrero, E. Zubía, M. J. Ortega, J. L. Carballo, *Bioorg. Med. Chem.* **2007**, *15*, 5275.
[25] M. R. Kernan, R. C. Cambie, P. R. Bergquist, *J. Nat. Prod.* **1990**, *53*, 615.
[26] K. Moody, R. H. Thomson, E. Fattorusso, L. Minale, G. Sodano, *J. Chem. Soc., Perkin Trans. 1* **1972**, 18.
[27] S. Nishiyama, S. Yamamura, *Bull. Chem. Soc. Jpn.* **1985**, *58*, 3453.
[28] Y. Okamoto, M. Ojika, S. Kato, Y. Sakagami, *Tetrahedron* **2000**, *56*, 5813.
[29] V. Costantino, E. Fattorusso, A. Mangoni, *J. Org. Chem.* **1993**, *58*, 186.
[30] R. E. Desjardins, C. J. Canfield, J. D. Haynes, J. D. Chulay, *Antimicrob. Agents Chemother.* **1979**, *16*, 710.
[31] W. Trager, J. B. Jensen, *Science* **1976**, *193*, 673.
[32] W. Van Huyssen, K. H. Rieckmann, *Trop. Med. Parasitol.* **1993**, *44*, 329.
[33] J. Lelièvre, A. Berry, F. Benoit-Vical, *Exp. Parasitol.* **2005**, *109*, 195.
[34] D. L. Pompliano, R. P. Gomez, N. J. Anthony, *J. Am. Chem. Soc.* **1992**, *114*, 7945.
[35] P. B. Cassidy, J. M. Dolence, C. D. Poulter, *Methods Enzymol.* **1995**, *250*, 30.
[36] L. Coudray, R. M. de Figueiredo, S. Duez, S. Cortial, J. Dubois, *J. Enzyme Inhib. Med. Chem.* **2009**, *24*, 972.
[37] C. Chombard, Ph.D. Thesis, Museum National d'Histoire Naturelle, Paris, 1998.
[38] G. Wörheide, *Facies* **1998**, *38*, 1.
[39] S. F. Altschul, W. Gish, W. Miller, E. W. Myers, D. J. Lipman, *J. Mol. Biol.* **1990**, *215*, 403.
[40] W. P. Maddison, D. R. Maddison, 'MacClade: Analysis of Phylogeny and Character Evolution', 3rd Edn., Sinauer Associates, Sunderland, Massachusetts, 1992.
[41] A. J. Drummond, B. Ashton, S. Buxton, M. Cheung, A. Cooper, C. Duran, M. Field, J. Heled, M. Kearse, S. Markowitz, R. Moir, S. Stones-Havas, S. Sturrock, T. Thierer, A. Wilson, Geneious v5.4, available from http://www.geneious.com, 2011.

Received September 23, 2011